Journal of Materials Chemistry C

Accepted Manuscript

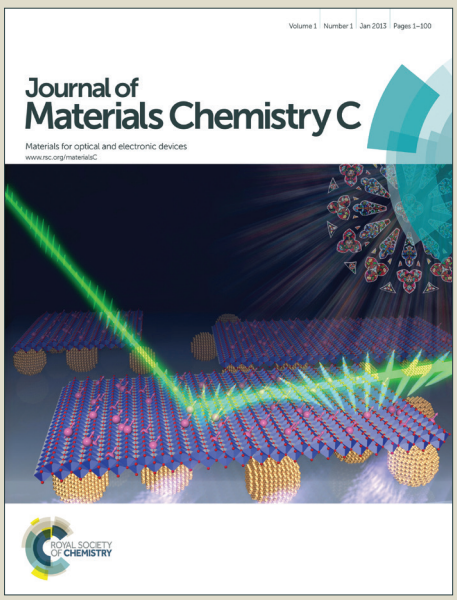

ROYAL SOCIETY OF CHEMISTRY

www.rsc.org/materialsC

Journal Name

RSCPublishing

ARTICLE

A high triplet energy, high thermal stability oxadiazole derivative as the electron transporter for highly efficient red, green and blue phosphorescent OLEDs

Cite this: DOI: 10.1039/x0xx00000x

Received , xx
Accepted , xx

DOI: 10.1039/x0xx00000x

www.rsc.org/

Cheng-Hung Shih, P. Rajamalli, Cheng-An Wu, Ming-Jai Chiu, Li-Kang Chu and Chien-Hong Cheng*

A high glass transition temperature (T_g = 220 °C), high triplet energy gap (E_T= 2.88 eV) and high electron mobility material bis(m-terphenyl)oxadiazole was readily synthesized. It can serve as a universal electron transporter for blue, green and red phosphorescent OLEDs with excellent efficiencies. The material shows high current density compared to the other electron transport materials and exhibits reduced driving voltage for all color PhOLEDs irrespective of the energy level of the host materials, due to efficient electron injection from 2,5-di([1,1':3',1"-terphenyl]-5'-yl)-1,3,4-oxadiazole (TPOTP) to host material. For the green PhOLED, a maximum external quantum efficiency (EQE) over 25%, current efficiency of 97.6 cd/A and power efficiency of 100.6 lm/W were achieved. The red and blue devices using TPOTP as the electron transporter also show EQE higher than 23% with very low roll-off in efficiencies in practical brightness level.

1 Introduction

Organic light-emitting diodes (OLEDs) have attracted great attention because of their applications in both flat and flexible displays and lighting.[1] Phosphorescent OLEDs are particularly fascinating due to the fact that their internal/external quantum efficiencies can be 4 times higher than the traditional fluorescence device.[2,3] To achieve excellent efficiencies, OLEDs are generally constructed with multilayers including anode, hole injection, hole-transporting, emissive (host and dopant), hole blocking, electron-transporting, electron injection and cathode layers.[4] For a RGB full-colour OLED display, a large number of materials should be used, if the red, green and red devices all use different materials. It would greatly simplify the manufacturing process and reduce the cost, if some of the materials can be shared with different devices to reduce the number of materials.

In the last few decades, many types of semiconducting hole transporting materials (HTM) and electron transporting materials (ETM) have been reported.[5] Among these two types of materials, Hole transporting semiconducting materials have become practical due to their high charge-carrier mobility and excellent operational durability.[6] Therefore, the development of ETM with high electron mobility are necessary to improve the OLED performance because the balance of hole and electron in a device is very important.[7] In addition, ETM should possess a high triplet energy gap to prevent dopant or host triplet excitons in the emissive layer to diffuse to the ET layer.[8] The ETM also should have an optimal lowest unoccupied molecular orbital (LUMO) energy level for the smooth electron injection from cathode to ETM and electron transport from ETM to the host layer and have the highest occupied molecular orbital (HOMO) level low enough to block the hole to get into the electron transporting layer.

There are many electron transport materials developed to reduce the driving voltage and improve efficiency of PhOLEDs.[9] Although the electron mobilities of these electron transport materials are improved, the LUMO levels are deep which are not suitable for electron injection into the common carbazole-based host materials with a shallow LUMO levels of 2.2 - 2.4 eV. Moreover, a high glass transition temperature for ETM is required to maintain the device stability. In general high T_g needs a rigid structure and high molecular weight. It is a great challenge to design a ETM having high T_g, and high energy gap as well, because these two properties are contradictory.

We are interested in synthesizing efficient thermally stable electron transport materials. Recently, we reported two oxadiazole-based ETMs for blue devices. Although these devices are efficient, their T_g and the electron mobility are

relatively low.[10] To improve these two properties, we designed and synthesized a new electron transporting material, 2,5-di([1,1':3',1"-terphenyl]-5'-yl)-1,3,4-oxadiazole (TPOTP). The oxadiazole unit was selected due to the advantages: i) high electron affinity; ii) wide energy gap; and iii) readily maintaining the planarity of the molecule. The meta-terphenyl unit was connected to enhance the thermal stability without much decrease of the energy gap. TPOTP possesses important properties such as high triplet energy, optimal HOMO and LUMO levels, high electron mobility and high T_g. This compound is utilized as a universal ETM for the phosphorescent blue, green and red OLEDs and all have achieved excellent device performance.

2 Results and discussion

2.1 Synthesis and characterization

As shown in Scheme 1, TPOTP could be synthesized from Suzuki coupling reaction of 2,5-bis(3,5-dibromophenyl)-1,3,4-oxadiazole (OBr_4) with phenyl boronic acid in good yield. One of the two starting materials, 5-(3,5-dibromophenyl)-1*H*-tetrazole (35Brtaz), was prepared from 3,5-dibromobenzonitrile and sodium azide in the presence of zinc chloride according to a literature procedure.[11] The details for the preparation of these compounds are given in the experimental section. This product was further purified by gradient temperature sublimation before device fabrication and was characterized by its ^1H, ^{13}C NMR, mass and elemental analysis data.

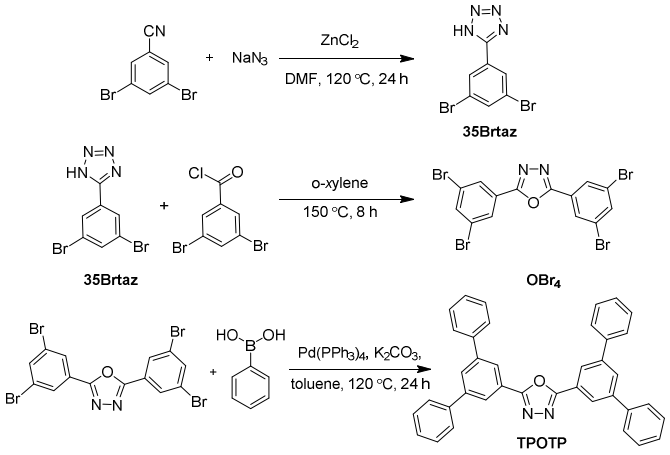

Scheme 1 Synthesis of TPOTP.

2.2 Photophysical properties

The UV-vis absorption and photoluminescence spectra at room temperature and at 77 K of TPOTP are shown in Fig. 1, whereas the peak maxima of these spectra are summarized in Table 1. The absorption peak appears at 260 nm in dichloromethane (10^{-5} M) solution and 267 nm in the thin-film, which can be attributed to π-π* transitions of the molecule (see Fig. 3 for the HOMO and LUMO). The fluorescence peak showed at 350 nm in dichloromethane (10^{-5} M) solution and 368 nm in the thin film. The observed red shift in the thin film state is likely due to the strong π-π stacking of the TPOTP molecules.

The singlet energy gap E_S of TPOTP as determined from the intersection of its absorption and emission spectra is 3.59 eV. The HOMO and LUMO energy levels were estimated to be 5.85 and 2.26 eV. The LUMO is calculated from the reduction potential (Fig. S1) and HOMO is determined from LUMO + E_S. The triplet energy gap (E_T) was estimated to be 2.76 eV, from the high energy peak of phosphorescent spectrum in the solid film at 77 K.

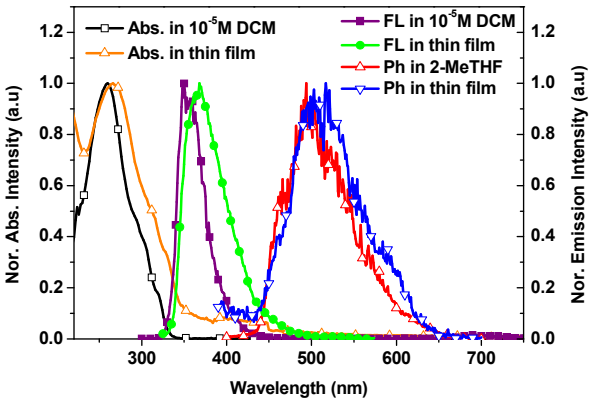

Fig. 1 The absorption (Abs.) and fluorescence (Fl.) spectra of TPOTP in dichloromethane (10^{-5} M) solution and thin film measured at room temperature; the phosphorescence (Ph) spectra measured in 2-MeTHF (10^{-5} M) and thin film at 77 K.

2.3 Thermal properties and DFT calculation

The thermal properties of TPOTP were determined by thermogravimetric analysis (TGA) and differential scanning calorimetry (DSC) measurement and the results are shown in Fig. 2 and Fig. S2. Even though TPOTP appears to be a simple molecule, it shows an extremely high glass transition temperature (T_g) of 220 °C much higher than the conventionally used ETL

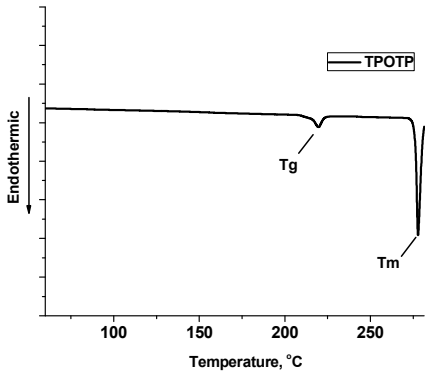

Fig. 2 Differential scanning calorimetry (DSC) trace of TPOTP with a scan rate of 10 °C/min.

Table 1 Physical and thermal properties of TPOTP

ETM	λ_{abs} (nm)[a]	λ_{abs} (nm)[b]	λ_{em} (nm)[a]	λ_{em} (nm)[b]	λ_{em} (nm)[c]	λ_{em} (nm)[d]	T_g (°C)[e]	T_m (°C)[e]	T_d (°C)[f]	LUMO (eV)[g]	HOMO (eV)[h]	E_g (eV)[i]	E_T(eV)[j]
TPOTP	260	267	350	368	461	489	220	278	425	2.26	5.85	3.59	2.76

[a]Measured in DCM (1×10^{-5} M) at room temperature. [b]Measured in thin film at room temperature. [c]Phosphorescence measured in 2-MeTHF (1×10^{-5} M) at 77 K. [d]Phosphorescence measured in thin film at 77 K. [e]Obtained from DSC measurements. [f]Obtained from TGA measurement. [g]Measured from the reduction potential in 10^{-3} M THF solution by cyclic voltammetry. [h]Measured from LUMO+E_g. [i]Estimated from the optical absorption threshold. [j]Estimated from the onset of phosphorescence spectrum.

materials such as BCP (80 °C) and TAZ (70 °C).[12] Also, it has a decomposition temperature (T_d) of 425 °C higher than that of OXD-7 (331 °C).[10] The high T_g of TPOTP suggests high morphologic stability of the amorphous phase in the film, an important property for the device. To gain insight into the electronic states of TPOTP, DFT calculation was performed. The results show that the HOMO is mostly distributed over the oxadiazole group and two central phenylene groups and to a less extent over the two peripheral phenyl groups (Fig. 3). Similar to the HOMO, the LUMO is also localized mainly on the oxadiazole moiety and the two central phenylene groups with negligible contribution from the four peripheral phenyls. Further, the HOMO, LUMO and triplet energy levels were estimated by the time-dependent density functional theory (TDDFT). The calculated HOMO and LUMO energy levels are 6.04 and 1.66 eV, respectively and the triplet energy gap is 2.75 eV. These values are in reasonable agreement with the experimental data in Table 1.

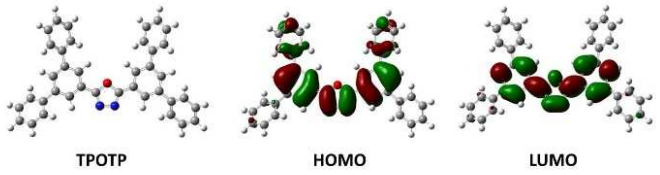

Fig. 3 Calculated spatial distributions of the HOMO and LUMO of TPOTP

To compare the electron transporting properties of this compound with other well-known transporting materials, several electron only devices using different EMTs were fabricated. These devices consist of the following structure: ITO/BCP (15 nm)/ ETM (40 nm)/LiF (1 nm)/Al (100 nm) where BCP = 2,9-dimethyl-4,7-diphenyl-1,10-phenanthroline. The current density vs voltage curves of these electron-only devices are shown in Fig. 4. TPOTP gave the lowest driving voltage and the highest current density at any applied voltage among the ET materials tested except TmPyPB. It is known that TmPyPB has very high electron mobility among the ETMs. However, TPOTP appears to have higher current density at low and high applied voltages than TmPyPB in the electron-only devices (Fig. 4). The results indicate that TPOTP is one of the highest electron mobility materials. The planar conformation, that would enhance the intermolecular π-π interaction, likely accounts for the high current density of the TPOTP-based device. Further, to see the exciton confinement within the emissive layer particularly for blue phosphorescent emitter, the transient PL decay of the TPOTP:Firpic (8%) doped thin film was measured under nitrogen atmosphere at room temperature. As shown in Fig S3, the film exhibits nearly mono-exponential decay with a lifetime of 1.5 μs.[13] The result suggests that the triplet energy of the TPOTP is large enough to prevent leakage of the blue phosphorescent triplet excitons to ETL.[13]

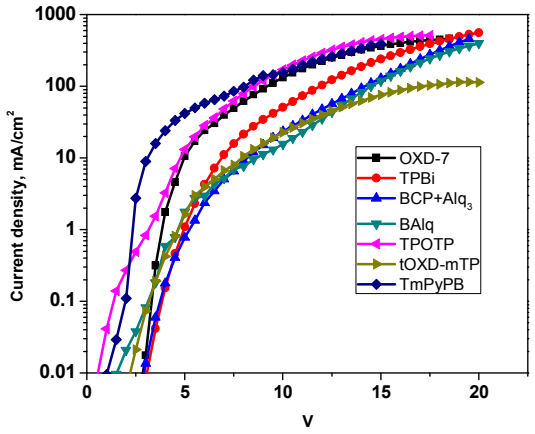

Fig. 4 Current density vs voltage characteristics of the electron-only devices.

To evaluate the performance of TPOTP as ETL, device G was fabricated using $Ir(ppy)_3$ as the dopant with the following device structure: ITO/NPB (20 nm)/ TCTA (10 nm)/BCPO: $Ir(ppy)_3$ (8% 30 nm)/TPOTP (40 nm)/LiF (1 nm)/Al (100 nm), where NPB = N^4,$N^{4'}$-di(naphthalen-1-yl)-N^4,$N^{4'}$-diphenylbiphenyl-4,4'-diamine and TCTA = 4,4′,4″-tris(*N*-carbazolyl)triphenylamine are hole-transporting materials and BCPO = 9,9'-(4,4'-(phenylphosphoryl)bis(4,1-phenylene))bis(9*H*-carbazole) is the host. The energy levels and the molecular structures of each layer in the device are shown in Fig. 5, while the performances of the device are summarized in Table 2. Device G shows a low turn-on voltage of 2.5 V, a remarkably external quantum efficiency, current efficiency, and power efficiency of 25.2%, 97.6 cd/A and 101 lm/W, respectively. In addition, the device gave a maximum luminance of 115000 cd m^{-2} with CIE of (x = 0.30, y = 0.64).

The current density-voltage and luminance-voltage curves are shown in Fig. 6a, while the EQE vs luminance curve is displayed in Fig. 6b. At a brightness level of 100 and 1000 cd m^{-2}, the external quantum efficiencies still retain as high as

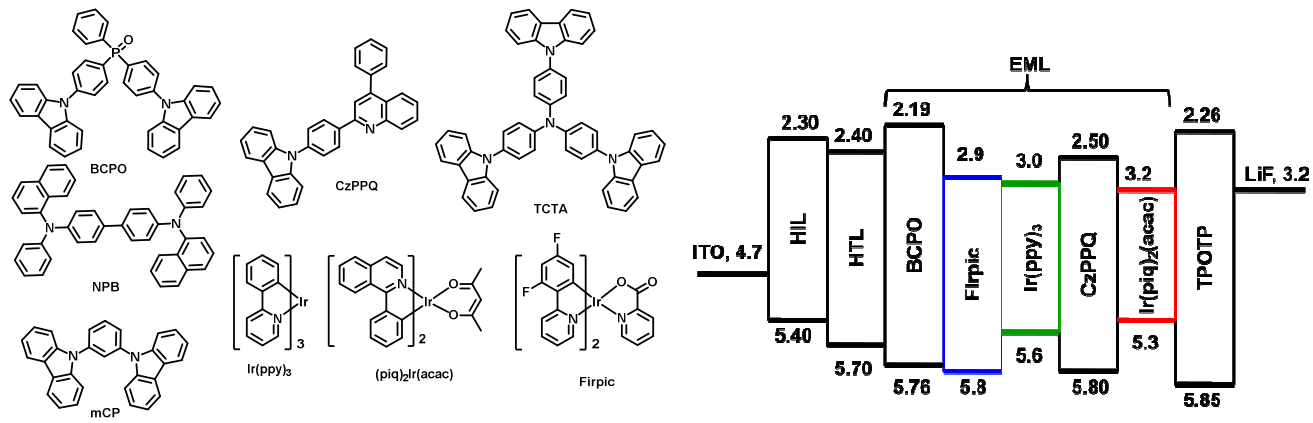

Fig. 5 The structures of the materials used and HOMO/LUMO levels in the EL devices

Table 2 EL performances of the devices with **TPOTP** as an ETM

Device[a]	V_d (V)[b]	L_{max} (cd/m^2, V)[c]	EQE_{max} (%, V)[c]	CE_{max}(cd/A, V)[c]	PE_{max} (lm/W, V)[c]	λ_{max}, (nm)[d] at 8V	CIE (x,y), at 8 V
G	2.5	115000, 16.5	25.2, 3.5	97.6, 3.5	101, 3.0	514	(0.30,0.64)
B	3.2	35600, 17.0	23.1, 4.0	49.1, 4.0	41.8, 3.5	472	(0.15,0.33)
R	3.0	38000, 17.5	23.6, 5.5	29.9, 5.5	20.2, 4.5	620	(0.67,0.33)

[a]Device configurations: device G – ITO/NPB (20 nm)/TCTA (10 nm)/BCPO: $Ir(ppy)_3$ (8 wt%) (30 nm)/ TPOTP (40 nm)/LiF (1 nm)/Al (100 nm); device B - ITO/NPB (30 nm)/*m*CP (20 nm)/BCPO: Firpic (8 wt%) (30 nm)/ TPOTP (40 nm)/LiF (1 nm)/Al (100 nm); device R - ITO/NPB (10 nm)/TCTA (20 nm)/CzPPQ: $(piq)_2Ir(acac)$ (4 wt%) (30 nm)/ TPOTP (30 nm)/LiF (1 nm)/Al (100 nm); [b]V_d, The operating voltage at a brightness of 1 cd/m^2; [c]L_{max}, Maximum luminance; EQE_{max}, Maximum external quantum efficiency; CE_{max}, Maximum current efficiency; PE_{max}, Maximum power efficiency; and [d]λ_{max}, The wavelength where the EL spectrum having the maximum intensity.

25.0% and 23.3%. To compare the device performance with conventional electron transporting materials, device G1 was fabricated using BCP and Alq_3 as an ETM and results are summarized in Table S1. Importantly, device G show higher EQE, power and current efficiency compared to those of the $Ir(ppy)_3$-based green device G1 using BCP and Alq_3.[8b] Our newly developed ETM not only possesses thermal stability, but also reduces the device complexity with improved efficiency. The EQE and current efficiency vs. luminance of this device is displayed in Figure 4b. Unlike previous reports,[14] this device shows low efficiency roll-off at higher current density. The EQE of device G at luminance 1000 cd m^{-2} retains 92.5% of their maximum values, indicating a balanced carrier recombination even at a high current density (Table S2).

In addition to the green phosphorescent OLED, TPOTP can also be applied as a ETL/EBL for blue and red phosphorescent devices. The commonly used Firpic and $Ir(piq)_2acac$ were selected as the blue and red dopant, respectively. The structures of blue and red devices are ITO/NPB (30 nm)/*m*CP (20 nm)/BCPO: FIrpic (8%) (30 nm)/TPOTP (40 nm)/LiF (1 nm)/Al (100 nm) and ITO/NPB (10 nm)/TCTA (20 nm)/ (CzPPQ): dopant (4% 30 nm)/TPOTP (30 nm)/LiF (1 nm)/Al (100 nm), respectively, where, CzPPQ = 9-(4-(4-phenylquinolin-2-yl)phenyl)-9H-carbazole is the host.[15] Here, 1,3-bis(9-*H*-carbazol-9-yl)benzene (*m*CP) is used as hole-transporting material and also as an exciton blocker to prevent diffusion of exciton to the NPB layer.

Device B (Table 2) reveals a low turn-on voltage of 3.2 V and high maximum external quantum efficiency, current efficiency and power efficiency of 23.1%, 49.1 cd/A, and 41.8 lm/W, respectively (Fig. 6). Moreover, a maximum luminance of 35600 cd/m^2 with CIE values of (0.15, 0.33) was reached. Interestingly, this device shows much improved performance (EQE-23.1% compared to the previously reported blue FIrpic device (EQE-11.4%) using OXD-7 as an ETM,[10] Device R exhibits a low turn-on voltage of 3.0 V, maximum external quantum efficiency, current efficiency and power efficiency of 23.6%, 29.9 cd/A, and 20.2 lm/W, respectively with maximum luminance 38000 cd m^{-2}. Devices B and R also show negligible roll-off similar to that of device G, at the practical brightness level of 100 and 1000 cd m^{-2}; the EQEs retain as high as 21.9% and 20.2% for device B and 23% and 23.2% for device R. The EQEs of devices B and R at luminance 1000 cd m^{-2} retain 92.2 and 98.3%, respectively (Table S2), of their maximum values, indicating a balanced carrier recombination even at a high current density. Although TPOTP possess shallow LUMO level, all devices show low turn-on voltages. This suggests that the electron injection from ETM to the host materials is very smooth and efficient. Since all these blue, green and red devices revealed high external quantum, current and power efficiencies. It is fascinating to mention that by using TPOTP as the

common EBL/ETL, the performance of these primary-color devices can be improved. To the best of our knowledge, this is the first report using a common ETL material for blue, green, and red phosphorescent devices with high performance.

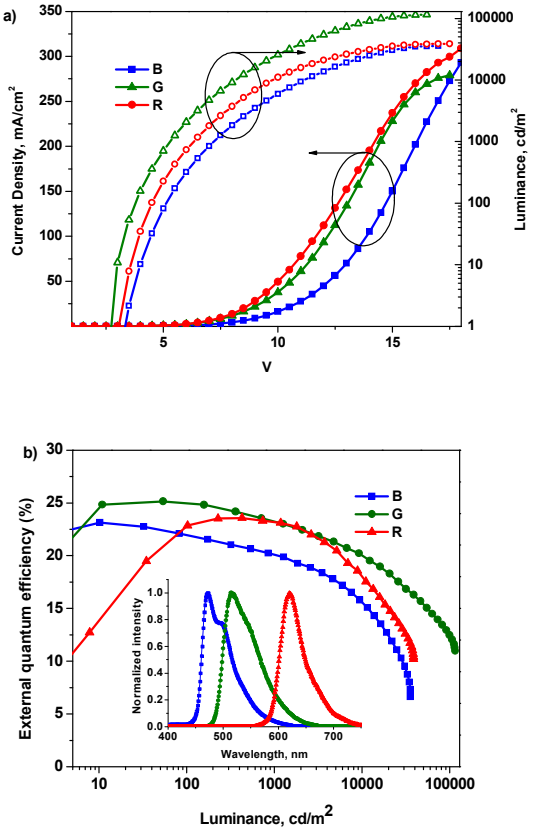

Fig. 6 a) Current density and luminance vs driving voltage, b) External quantum efficiency vs luminance and inset: luminance spectra of B, G and R.

3 Conclusion

In summary, a new highly thermally stable (T_g = 220 °C) and high triplet energy gap (E_T = 2.76 eV) with shallow LUMO level oxadiazole based ET material, TPOTP, was synthesized. The material was used as a universal electron transporter/exciton blocker for blue, green and red phosphorescent devices. The material effectively transports electrons and blocks the holes and excitons and improves the charge balance in the EML of the devices, resulting in high device efficiencies for all of the devices, particularly the green one with an EQE of 25.2%, current efficiency of 97.6 cd/A and power efficiency of 100.6 lm/W. Moreover, all devices show very low efficiency roll-off in the practical ranges.

4 Experimental section

4.1 General information

UV-vis absorption spectra were recorded using a Hitachi U-3300 spectrophotometer. PL spectra and phosphorescent spectra were measured on a Hitachi F-4500 spectrophotometer. The electrochemical properties were measured by 600s A CH Instruments. The HRMS were measured on a MAT-95XL HRMS. Elemental analysis was measured on an Elementar vario EL III. The glass transition temperature was determined by DSC under nitrogen atmosphere using a DSC-Q10 instrument. The decomposition temperature was determined by TGA using TG/DTA Seiko SSC-5200 instrument. The molecular geometry optimizations and electronic properties were computed by carrying out the Gaussian 03 program with density functional theory (DFT) and time-dependent DFT (TDDFT) calculations, in which the Becke's three-parameter functional combined with Lee, Yang, and Parr's correlation functional (B3LYP) hybrid exchange-correlation functional with the 6-31G* basic set were used. The molecular orbitals were visualized on the Gaussview 4.1 software.

4.2 Synthesis of 5-(3,5-dibromophenyl)-1*H*-tetrazole (35Brtaz)[11a]

To a 250 mL round-bottom flask, 3,5-dibromo benzonitrile (15.65 g, 60.0 mmol), sodium azide (7.8 g, 120 mmol), zinc chloride (16.35 g, 120 mmol), and 100 mL of DMF was added. The reaction mixture was stirred at 120 °C for 24 h. After completion, the reaction was cooled to room temperature and then poured into 1N HCl solution (300 mL). The precipitated solid was filtered and washed with water. After dried under vacuum, white solid 35Brtaz was obtained in 70% yield. Expected product was confirmed by ^{1}H and ^{13}C NMR spectroscopy. ^{1}H NMR (400 MHz, DMSO-d_6, δ): 8.12 (s, 2H), 7.92 (s, 1H); ^{13}C NMR (100 MHz, DMSO-d_6, δ): 155.5, 135.0, 129.6, 128.4, 123.2.

4.3 Synthesis of 2,5-bis(3,5-dibromophenyl)-1,3,4-oxadiazole (OBr_4)[11b]

A mixture of 5-(3,5-dibromophenyl)-1*H*-tetrazole (20.0 mmol), 3,5-dibromobenzoyl chloride (22.0mmol) in *o*-xylene (50 mL) was refluxed for 8 h under nitrogen atmosphere. After completion, the reaction mixture was cooled to room temperature and the solvent was removed under reduced pressure and recrystallized from *n*-hexane to give white solid OBr_4 in 65% yield. The desired product was confirmed by ^{1}H NMR spectroscopy and mass spectrometry. ^{1}H NMR (400 MHz, $CDCl_3$, δ): 8.20 (d, J = 2 Hz, 4H), 7.85 (t, J = 2 Hz, 2H); HRMS (m/z): [M^+] calcd. for $C_{14}H_6Br_4N_2O$, 533.7214; found, 533.7216.

4.4 Synthesis of 2,5-di([1,1':3',1''-terphenyl]-5'-yl)-1,3,4-oxadiazole (TPOTP)

$Pd(PPh_3)_4$ (346 mg, 0.30 mmol) was added under nitrogen atmosphere to the solution of OBr_4 (2,5-bis(3,5-dibromophenyl)-1,3,4-oxadiazole) (5.34 g, 10.0 mmol), phenylboronic acid (5.5 g, 45.0 mmol) and K_2CO_3 (9.3 g, 67.7 mmol) in toluene (90 mL), ethanol (40 mL) and water (40 mL) solvent mixture. Then, the reaction mixture was heated at 120 °C for 24 h under nitrogen atmosphere. After completion, the reaction mixture was cooled to room temperature and poured into water to precipitate the product and filtered. The crude

product was dissolved in dichloromethane and washed with water. The organic layer was concentrated under reduced pressure and the residue was purified by a silica gel column chromatography using dichloromethane/methanol mixture (20:1, v/v) as the eluent to give a white solid TPOTP in 70% yield. Product was confirmed by ^{1}H and ^{13}C NMR spectroscopy and mass spectrometry. ^{1}H NMR (400 MHz, $CDCl_3$, δ): 8.35 (s, 4H), 7.97 (s, 2H), 7.72 (d, 8H), 7.50 (t, J = 7.4 Hz, 8H), 7.42 (t, J = 7.2 Hz, 4H); ^{13}C NMR (100 MHz, $CDCl_3$, δ): 164.77, 142.87, 139.91, 129.41, 129.00, 128.08, 127.35, 124.85, 124.45; HRMS (m/z): [M+] calcd. for $C_{38}H_{26}N_2O$, 526.2045; found, 526.2042; Anal. calcd. for $C_{38}H_{26}N_2O$: C 86.67, H 4.98, N 5.32, O 3.04; Found: C 86.50, H 5.01, N 5.34, O 3.15.

4.5 OLEDs fabrication and measurement

Organic chemicals used for fabricating devices were purified by temperature gradient vacuum sublimation. The EL devices were fabricated by vacuum deposition of the materials at a base pressure less than 10^{-6} Torr onto a glass pre-coated with a layer of ITO with a sheet resistance of 25 Ω/square. The deposition rate for organic compounds is 0.5~3 Å s^{-1}. The cathode consisting of LiF/Al was deposited by evaporation of LiF with a deposition rate of 0.1 Å s^{-1} and then by evaporation of Al metal with a rate of 3~10 Å s^{-1}. The active area of the devices is 9 mm^2. The EL spectra were taken with a Hitachi F-4500 fluorescence spectrophotometer. The measurements of current, voltage and luminance were made simultaneously in the air using a Keithley 2400 source meter and a Topcon BM-7 luminance meter. The external quantum efficiencies of the prepared devices were calculated from the EL spectrum, luminance and current density.

Acknowledgements

We thank Ministry of Science and Technology of Republic of China (MOST-102-2633-M-007-002) for support of this research.

Notes and references

Department of Chemistry, National Tsing Hua University, Hsinchu 30013, Taiwan, Fax: 886-3-572469, Tel: 886-3-5721454. E-mail: chcheng@mx.nthu.edu.tw

† Electronic Supplementary Information (ESI) available: CV, TGA, device performance and characterization data. See DOI: 10.1039/b000000x/

1 (a) J.-H. Choi, K.-H. Kim, S.-J. Choi and H. H. Lee, *Nanotechnology*, 2006, **17**, 2246; b) Y. Nakajima, T. Takei, T. Tsuzuki, M. Suzuki, H. Fukagawa, T. Yamamoto and S. Tokito, *J. Soc. Inf. Disp.*, 2009, **17**, 629; c) K. T. Kamtekar, A. P. Monkman and M. R. Bryce, *Adv. Mater.*, 2010, **22**, 572; d) J. Kido, M. Kimura and K. Nagai, *Science*, 1995, **267**, 133; e) H. B. Wu, L. Ying, W. Yang and Y. Cao, *Chem. Soc. Rev.*, 2009, **38**, 3391; f) M. A. Baldo, M. E. Thompson and S. R. Forrest, *Nature*, 2000, **403**, 750; g) H.-H. Chou, H.-H. Shih and C.-H. Cheng, *J. Mater. Chem.* 2010, **20**, 798; h) H.-H. Chou and C.-H. Cheng, *Adv. Mater.* 2010, **22**, 2468; i) Y.-H. Chen, H.-H. Chou, T.-H. Su, P.-Y. Chou, F.-I. Wu and C.-H. Cheng, *Chem. Commun.* 2011, **47**, 8865; j) C.-H. Fan, P. Sun, T.-H. Su and C.-H. Cheng, *Adv. Mater.* 2011, **23**, 2981.

2 a) M. A. Baldo, D. F. ÓBrien, Y. You, A. Shoustikov, S. Sibley, M. E. Thompson and S. R. Forrest, *Nature*, 1998, **395**, 151; b) T.-H. Su, C.-H. Fan, Y.-H. O.-Yang, L.-C. Hsu and C.-H. Cheng, *J. Mater. Chem. C*, 2013, **1**, 5084; c) Y. Tao, C. Yang and J. Qin, *Chem. Soc. Rev.*, 2011, **40**, 2943; d) K. S. Yook and J. Y. Lee, *Adv. Mater.* 2012, **24**, 3169; e) H. Sasabe and J. Kido, *Eur. J. Org. Chem.* 2013, 7653.

3 a) J.-J. Lin, W.-S. Liao, H.-J. Huang, F.-I. Wu and C.-H. Cheng, *Adv. Funct. Mater.* 2008, **18**, 485; b) K.-Y. Lu, H.-H. Chou, C.-H. Hsieh, Y.-H. O. Yang, H.-R. Tsai, H.-Y. Tsai, L.-C. Hsu, C.-Y. Chen, I.-C. Chen and C.-H. Cheng, *Adv. Mater.* 2011, **23**, 4933; c) C.-H. Hsieh, F.-I. Wu, C.-H. Fan, M.-J. Huang, K.-Y. Lu, P.-Y. Chou, Y.-H. O. Yang, S.-H. Wu, I.-C. Chen, S.-H. Chou, K.-T. Wong and C.-H. Cheng, *Chem. Eur. J.* 2011, **17**, 9180.

4 a) C. W. Tang and S. A. VanSlyke, *Appl. Phys. Lett.*, 1987, **51**, 913; b) C. Adachi, T. Tsutsui and S. Saito, *Appl. Phys. Lett.*, 1990, **57**, 531.

5 H. Tanaka, S. Tokito, Y. Taga and A. Okada, *Chem. Commun.*, 1996, 2175.

6 Z. Jiang, Z. Liu, C. Yang, C. Zhong, J. Qin, G. Yu and Y. Liu, *Adv. Funct. Mater.*, 2009, **19**, 3987.

7 a) N. Chopra, J. Lee, Y. Zheng, S.-H. Eom, J. Xue and F. So, *Appl. Phys. Lett.*, 2008, **93**, 143307; b) Y. Li, M. K. Fung, Z. Xie, S. T. Lee, L.-S. Hung, J. Shi and Y. Q. Li, *Adv. Mater.*, 2002, **14**, 1317.

8 a) Y. Sun, N. C. Giebink, H. Kanno, B. Ma, M. E. Thospson and S. R. Forrest, *Nature*, 2006, **440**, 908; b) N. Matsusue, S. Ikame, Y. Suzuki and H. Naito, *J. Appl. Phys.*, 2005, **97**, 123512; c) H. Choukri, A. Fischer, S. Forget, S. Chénais, M.-C. Castex, D. Adès, A. Siove and B. Geffroy, *Appl. Phys. Lett.*, 2006, **89**, 183513.

9 a) M. Liu, S.-J. Su, M.-C. Jung, Y. Qi, W.-M. Zhao and J. Kido, *Chem. Mater.* 2012, **24**, 3817; b) S.-J. Su, T. Chiba, T. Takeda and J. Kido, *Adv. Mater.*, 2008, **20**, 2125; c) L. Xiao, X. Xing, Z. Chen, B. Qu, H. Lan, Q. Gong and J. Kido, *Adv. Funct. Mater.*, 2013, **23**, 1323; d) A. P. Kulkarni, C. J. Tonzola, A. Babel and S. A. Jenekhe, *Chem. Mater.* 2004, **16**, 4556; e) S. O. Jeon, K. S. Yook, C. W. Joo and J. Y. Lee, *J. Mater. Chem.*, 2009, **19**, 5940.

10 C.-A. Wu, H.-H. Chou, C.-H. Shih, F.-I. Wu, C.-H. Cheng, H.-L. Huang, T.-C. Chao and M.-R. Tseng, *J. Mater. Chem.*, 2012, **22**, 17792.

11 a) F. Himo, Z. P. Demko, L. Noodleman, K. B. Sharpless, *J. Am. Chem. Soc.*, 2002, **124**, 12210; b) Z. P. Demko, K. B. Sharpless, *J. Org. Chem.*, 2001, **66**, 7945.

12 a) M.-H. Tsai, H.-W. Lin, H.-C. Su, T.-H. Ke, C.-C. Wu, F.-C. Fang, Y.-L. Liao, K.-T. Wong and C.-I. Wu, *Adv. Mater.*, 2006, **18**, 1216; b) T. Yasuda, Y. Yamaguchi, D.-C. Zou and T. Tsutsui, *Jpn. J. Appl. Phys.*, 2002, **41**, 5626.

13 S. Tokito, T. Iijima, Y. Suzuri, H. Kita, T. Tsuzuki, F. Sato, *Appl. Phys. Lett.* 2003, **83**, 569.

14 L. Xiao, S.-J. Su, Y. Agata, H. Lan and J. Kido, *Adv. Mater.* 2009, **21**, 1271.

15 C.-H. Chen, L.-C. Hsu, P. Rajamalli, Y.-W. Chang, F.-I. Wu, C.-Y. Liao, M.-J. Chiu, P.-Y. Chou, M.-J. Huang, L.-K. Chu and C.-H. Cheng, *J. Mater. Chem. C*, 2014, **2**, 6183.

TOC graphics:

A high triplet energy, high thermal stability oxadiazole derivative as the electron transporter for highly efficient red, green and blue phosphorescent OLEDs

Cheng-Hung Shih, P. Rajamalli, Cheng-An Wu, Ming-Jai Chiu, Li-Kang Chu and Chien-Hong Cheng*

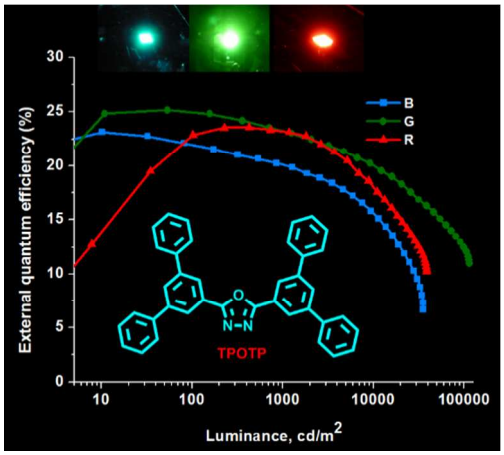

A high glass transition, triplet energy gap and electron mobility material, a bis(*m*-terphenyl)oxadiazole derivative TPOTP, is readily synthesized. It can serve as an efficient universal electron transporter and exciton blocker for blue, green and red phosphorescent OLEDs with maximum external quantum efficiencies all exceeding 23%.